Title page

Title

ITGB4 promotes the progression of colorectal cancer by activating Wnt/β-catenin signaling pathway via targeting EZR

Authors' names

Jing Wang[1#], Yi Si[1#], Mingda Xuan[1#], Shuangshuang Han[1], Kunyi Liu[1], Jiao Jiao[1], XiaoYan Men[1], HongFei Li[1], Weifang Yu[1*], Ting Liu[1*], Jia Wang[2*]

[1] Department of Endoscopy Center, The First Hospital of Hebei Medical University, Shijiazhuang, China

[2] Department of Infectious Diseases, The First Hospital of Hebei Medical University, Shijiazhuang, China

[#] These authors contributed equally

[*]The corresponding authors

Running title

ITGB4 promotes CRC by regulating EZR and Wnt/β-catenin signaling pathway

Corresponding author: Weifang Yu, M.D., Professor, No. 89 Donggang Road, Shijiazhuang, Hebei, China. E-mail: yuweifang@hebmu.edu.cn. Ting Liu, No. 89 Donggang Road, Shijiazhuang, Hebei, China. E-mail: 59103696@hebmu.edu.cn. Jia Wang, Professor, No. 89 Donggang Road, Shijiazhuang, Hebei, China. E-mail: 57101040@hebmu.edu.cn

Keywords: ITGB4 (Integrin Beta 4)；EZR (Ezrin)；Colorectal Cancer；Cell Biology；Wnt/β-catenin Signaling Pathway

Abstract

Background: Integrin Beta 4 (ITGB4), a member of the integrin family, was found to be abnormally highly expressed in colorectal cancer tissues and serum in our previous research, and it was associated with clinicopathological types and overall survival. This study further explores the potential mechanisms of ITGB4 in the occurrence and development of colorectal cancer, seeks downstream target genes and signaling pathways, and provides new insights for precision treatment of colorectal cancer.

Methods: Through bioinformatics analysis, it was verified that ITGB4 and EZR are highly expressed in tumor tissues of CRC patients and are associated with poor patient prognosis. The effects of ITGB4 on the proliferation, migration, invasion, and apoptosis of CRC cells were validated using CCK-8, wound healing assay, Transwell migration, and invasion assays. A nude mouse tumor formation experiment was conducted to validate the tumor-promoting effect of ITGB4 in vivo. Transcriptome sequencing was performed in SW480 cells with ITGB4 knockdown, and potential downstream targets and signaling pathways of ITGB4 were screened using KEGG enrichment analysis and bioinformatics analysis. The interaction between ITGB4 and downstream target genes was further demonstrated by immunofluorescence co-staining and co-immunoprecipitation. Key proteins in the downstream signaling pathway (β-catenin, c-Myc, and cyclinD1) were detected by Western blot to clarify the potential signaling pathway through which ITGB4 functions in CRC. Rescue experiments were conducted to validate the role of ITGB4 and its downstream target genes in the proliferation, migration, and invasion of colorectal cancer.

Results:ITGB4 is highly expressed in CRC tissues and cells. In vitro, downregulation of ITGB4 can inhibit the proliferation, migration, and invasion of CRC cells and promote apoptosis. In vivo, ITGB4 contributes to the growth of CRC tumor tissues and regulates the tumorigenic properties such as proliferation and invasion of CRC cells. Additionally, EZR has been preliminarily identified as a key downstream target of ITGB4, as the effects of ITGB4 knockdown on the proliferation, migration, and invasion of CRC cells can be rescued by overexpressing EZR. We also demonstrated that the ITGB4/EZR axis promotes the occurrence and development of CRC by activating the Wnt/β-catenin signaling pathway and regulating various biological functions of CRC cells.

Conclusions:ITGB4 targets and regulates EZR, and by activating the Wnt/β-catenin signaling pathway, it affects the proliferation, migration, and invasion of CRC, suggesting that ITGB4 may become a potential biomarker and therapeutic target.

Introduction

Colorectal cancer (CRC) is one of the most common intestinal tumors worldwide. It ranks third in the incidence of all malignant tumors globally and is the second leading cause of cancer-related deaths [1]. Currently, the treatment for colorectal cancer often involves a combination of surgery, radiotherapy, and chemotherapy, but the efficacy is limited[2-3]. Therefore, the search for new therapeutic targets to inhibit the proliferation, invasion, and migration of colorectal cancer cells has become a research focus in recent years. With the establishment of public biological databases for colorectal cancer and the development of bioinformatics, multiple studies have shown that gene

mutations play a crucial role in the occurrence and development of colorectal cancer[4]. In-depth research on abnormal genes, understanding the mechanisms of occurrence and development of colorectal cancer, and identifying potential biomarkers and therapeutic targets are vital for the early diagnosis and precise treatment of colorectal cancer.

Previously, supported by a national-level project from the Ministry of Science and Technology, our research group has utilized internationally leading mass cytometry (CyTOF) technology, gene chip, and protein chip technology to screen out a gene of significant value in the diagnosis and treatment of colorectal cancer—ITGB4. This achievement has been granted a national invention patent (Patent Number: ZL 2017 1 1148747.1) [5].Integrin β4 (integrin beta 4, ITGB4) is a member of the integrin family and is primarily expressed on the basal membrane side of epithelial cells.Some studies have shown that ITGB4 is highly expressed in breast cancer, bladder cancer, cervical cancer, head and neck cancer, lung cancer, and pancreatic cancer, and is associated with tumor invasion and poor prognosis [7-8]. Our team's previous research has found that ITGB4 is abnormally highly expressed in colorectal cancer tissues and serum, and it is related to clinical pathological types and overall survival. After annotating the ITGB4 co-expressed genes, it was found that multiple signaling pathways, including cell growth, cell migration, and apoptosis signaling, may be involved in the regulation of ITGB4 on the progression of colon cancer [6,16]. However, its mechanism of action in colorectal cancer is not yet clear.Therefore, the impact of ITGB4 on tumor initiation and the development of colorectal cancer (CRC), as well as the downstream

target genes of ITGB4 and the mechanisms of interaction, and the exploration of signaling pathways are the focus of this study.

In this study, we investigated the effects of ITGB4 knockdown on the proliferation, invasion, and apoptosis of human colorectal cancer (CRC) cells in vitro. We also observed the impact of ITGB4 on tumor malignant phenotypes in vivo. Through RNA-seq detection and bioinformatics analysis, we first confirmed the downstream target gene EZR of ITGB4 in CRC, which is highly expressed in CRC tumor tissues and has an interacting relationship with ITGB4. ITGB4 directly targets and promotes the expression level of EZR and plays a carcinogenic role in the pathogenesis of colorectal cancer by regulating EZR and activating the Wnt/β-catenin signaling pathway. These findings suggest that the ITGB4/EZR axis is an important regulatory factor in the development of CRC and provides a potential target for precision therapy in CRC.

Materials and Methods

Cell Culture

The human colorectal cancer cell lines SW480 and HCT116 were purchased from ATCC. SW480 and HCT116 cells were cultured in DMEM (Gibco) medium supplemented with 10% fetal bovine serum under a fully humidified environment at a constant temperature of 37°C and 5% CO2. The cells used in the experiments were all in the logarithmic growth phase with good viability.

siRNAs, shRNAs, Transfections and Stable cell lines

110 The logarithmically growing SW480 cells and HCT116 cells in good condition were
111 seeded into a 6-well plate at a density of 1×105 cells/ml. Transfection was performed
112 according to Lipofectamine 3000 (Invitrogen, Carlsbad, CA, USA) when the cell
113 confluence reached 80-90% in a cell culture flask or dish. ITGB4 siRNA and negative
114 control (GenePharma Co., Ltd., Shanghai, China) were transfected into SW480 and
115 HCT116 cells, while an EZR overexpression plasmid and negative control
116 (GenePharma) were transfected into SW480 and HCT116 cells, respectively. At the
117 same time, ITGB4 shRNA and negative control (shNC; GenePharma) were
118 transfected into SW480 cells to construct a stable transfection cell line. After
119 transfecting shITGB4 and shNC into the SW480 cell line for 48 hours, the culture
120 medium was replaced with medium containing the optimal concentration of 600
121 μg/ml neomycin (without other antibiotics). The culture medium was replaced every
122 2-3 days based on cell growth and medium color. When a significant number of cells
123 died, the concentration of neomycin was reduced to 300 μg/ml, and the selection was
124 continued for 10 days. Resistant cell clones in clusters became visible, and the drug
125 was then withdrawn for routine culture. The knockdown efficiency was verified.

126 **RNA extraction and qRT-PCR**

127 Total cellular RNA is extracted according to the instructions of RNA-Easy (Vazyme
128 Biotech Co., Ltd., Nanjing, China). RNA is reverse-transcribed into cDNA using the
129 PrimeScript RT Reagent Kit (Takara, Beijing, China) strictly following the
130 manufacturer's instructions, followed by PCR amplification. The amplification
131 program is: 95°C for 5 minutes; 95°C for 10 seconds, 60°C for 30 seconds, for a total

132 of 40 cycles. All experiments are conducted using the 4800 Real-Time Quantitative
133 PCR System.The sequence of primers are detailed in Supplementary Table 1.

134 **Western blot analysis and antibodies**

135 Proteins were digested and extracted using RIPA lysis buffer (Solarbio) and protease
136 inhibitor PMSF (Solarbio) in a ratio of 100:1. The proteins were separated
137 electrophoretically on a 10% SDS polyacrylamide gel (Bio-Rad Laboratories Inc,
138 Hercules, CA, USA) and transferred to a polyvinylidene fluoride membrane (Merck
139 Millipore, Billerica, MA, USA). The antibodies used in this study include: ITGB4
140 antibody (diluted 1:1000; Abcam, Cambridge, MA, USA; Catalog number: ab261778),
141 β-actin antibody (diluted 1:1500; ZSBG-Bio; Catalog number: TA-09), EZR antibody
142 (diluted 1:1000; Proteintech, Wuhan, Hubei; Catalog number: 26056-1-AP),
143 β-Catenin antibody (diluted 1:1000; Proteintech, Wuhan, Hubei; Catalog number:
144 51067-2-AP), c-Myc antibody (diluted 1:1000; Proteintech, Wuhan, Hubei; Catalog
145 number: 10828-1-AP), and Cyclin D1 antibody (diluted 1:500; Proteintech, Wuhan,
146 Hubei; Catalog number: 60186-1-Ig). The immune-reactive protein bands were
147 detected using the Odyssey scanning system (LI-COR Biosciences, Lincoln, NE,
148 USA). Quantitative analysis of the obtained images was performed using ImageJ
149 image analysis software. All samples were tested in triplicate.

150 **Cell proliferation assay**

151 The CCK-8 proliferation assay involved seeding cells into a 96-well plate at a density
152 of 1×10^3 cells per well and culturing them in complete medium containing 10% fetal
153 bovine serum. At 24, 48, 72, and 96 hours after cultivation, 10 μl of Cell Counting

154 Kit-8 (CCK-8; Dojindo, Tokyo, Japan) reagent was added to each well. The plate was
155 then incubated in a cell culture incubator for 2 hours. The absorbance at 450 nm for
156 each well was measured using a Promega GloMax luminescent detector (Promega,
157 Madison, WI, USA).
158 The clonogenic assay involved seeding cells from each group into a 6-well plate at a
159 density of 500 cells per well. The culture medium was replaced every three days, and
160 the cells were cultured for 10-14 days. After the incubation period, the cells were
161 washed twice with PBS, fixed with 4% paraformaldehyde for 30 minutes, and stained
162 with 0.1% crystal violet for 20 minutes. The number of clones with more than 50 cells
163 was counted under a microscope.
164 **Cell migration assay**
165 The wound healing assay was conducted by seeding cells from each group evenly into
166 a 6-well plate and culturing them in complete medium containing 10% fetal bovine
167 serum until the cell confluence approached 100%. A straight line wound was created
168 in the bottom of each well using the tip of a 200 μl pipette, mimicking a wound. The
169 cells were then washed twice with PBS to remove any debris, and the culture was
170 continued with serum-free medium. Images of each well were taken at 0 hours and 48
171 hours after the scratch was made. The migration rate was calculated as the ratio of the
172 gap width measured at 48 hours to the gap width measured at 0 hours.
173 The Transwell migration assay involves resuspending the cells from each group in
174 serum-free medium and then seeding 200 μl of the cell suspension, containing 1×10^5
175 cells, into the upper chamber (Corning Incorporated, Corning, NY, USA). The lower

chamber is filled with 700 μl of complete medium containing 10% fetal bovine serum to induce cell migration downward. After incubating in the incubator for 48 hours, the chamber was removed, washed twice with PBS, and then immersed in a well containing 700 μl of pre-cooled 4% paraformaldehyde for 30 minutes of fixation at room temperature. The chamber was then transferred to a well with 700 μl of 0.1% crystal violet staining solution and stained for 20 minutes at room temperature. The excess crystal violet was cleaned again with PBS. Five visual fields were randomly selected for photography, and the stained cells were counted using ImageJ software (National Institutes of Health, Bethesda, MD, USA).

Cell invasion assay

The Transwell invasion assay involves resuspending the cells from each group in serum-free medium, then adding 100 μl of the cell suspension containing 1×105 cells to the upper chamber. The lower chamber is filled with 700 μl of complete medium containing 10% fetal bovine serum to induce cell invasion downward. The remaining process and conditions are the same as those in the Transwell migration assay.

Cell apoptosis assay

The apoptosis of cells was detected using the Annexin V and PI double staining method. After 48 hours of transfection, the cells from each group were stained according to the instructions of the Annexin V9-FITC/PI Apoptosis Assay Kit (NeoBioscience, Shenzhen, China). Flow cytometry (BD Biosciences, San Jose, CA, USA) was used to analyze the apoptosis, and the percentage of apoptotic cells was calculated using FlowJo software.

198 **Animal studies**

199 Cells in the logarithmic growth phase from the transfection group (shITGB4) and the
200 control group (shNC) were digested with 0.25% trypsin to prepare a single-cell
201 suspension. The cell concentration was adjusted to 1×107/ml using serum-free
202 DMEM medium. Male nude mice, 5 weeks old, were also divided into a transfection
203 group and a control group, with 6 mice in each group. The cells from both groups
204 were inoculated subcutaneously into the nude mice at a dose of 0.2 ml per mouse.
205 Tumor formation was observed 3 days later, and tumor size was monitored every 3
206 days. Tumor formation was considered to have occurred when the subcutaneous
207 tumor nodules reached 1000 mm3. The long and short diameters of the tumors were
208 measured, and a tumor growth curve was plotted. Two weeks later, all animals were
209 euthanized by cervical dislocation, and the tumor weights were measured. The
210 volume of the transplanted tumors was calculated using the following formula: Tumor
211 volume (V) = (long diameter × short diameter2) / 2.

212 **RNA sequencing (RNA-seq)**

213 The siRNA-ITGB4 and siRNA-NC were transfected into SW480 cells, and total RNA
214 was extracted 24 hours later. The construction of the RNA library and sequencing
215 analysis were outsourced to Novogene Technology Co., Ltd. The Illumina NovaSeq
216 6000 platform was used to test 6 groups of samples (siNC×3, siITGB4×3). The output
217 data from each sample were subjected to quality control and filtering to obtain
218 high-quality data. The high-quality data were aligned to the reference genome using
219 the HISAT software, and the expression levels of genes or transcripts in the samples

220 were quantitatively analyzed. Differential expression analysis was performed using
221 the DESeq2 software, and genes with a log2|Fold Change| > 1.0 and P < 0.05 were
222 defined as differentially expressed genes.

223 **Immunohistochemistry (IHC)**

224 Tissues from nude mice were fixed with 4% paraformaldehyde, followed by paraffin
225 embedding (Shanghai YiYang Instrument Co., Ltd., Shanghai, China), sectioning, and
226 staining. The Rabbit/Mouse two-step detection kit (Beijing ZSBG-Bio Co., Ltd.,
227 Beijing, China) was used for immunohistochemical analysis according to the was
228 used for immunohistochemical analysis according to the manufacturer's instructions.
229 Anti-Ki67 (diluted 1:100; Proteintech; Catalog number: 27309-1-AP) antibodies were
230 used for immunohistochemical staining. The staining results were analyzed by using
231 the average optical density (AOD) method.

232 **Co-Immunofluorescent (Co-IF) assay**

233 Place cover glasses in a six-well plate and seed SW480 cells evenly on top. When the
234 cell confluence reaches 20%-30%, gently wash the cells three times with PBS, fix the
235 cells with 4% paraformaldehyde, permeabilize with 0.2% Triton X-100 (Solarbio;
236 Catalog number: T8200), and block with 2% bovine serum albumin (BSA-V; Solarbio;
237 Catalog number: A8020). Incubate the cells with ITGB4 antibody (1:50 SANTA
238 CRUZ, sc-13543) and EZR antibody (1:50 Proteintech, Wuhan, Hubei, 26056-1-AP)
239 overnight at 4°C. Then, incubate with fluorescently labeled secondary antibodies
240 (diluted 1:500; Cy3 anti-rabbit IgG, FITC anti-mouse IgG; Beyotime Biotechnology
241 Co., Shanghai, China) at room temperature in the dark for 1 hour. Stain the cell nuclei

242 with 4’,6’-diamino-2-phenylindole dihydrochloride (DAPI; Beyotime Biotechnology
243 Co.). Take photographs using a laser scanning confocal microscope (ZEISS,
244 Oberkochen, Germany).

245 **Co-Immunoprecipitation (Co-IP) assay**

246 Take SW480 cells in the logarithmic growth phase and gently wash them twice with
247 PBS. Cell lysis and immunoprecipitation (IP) are performed according to the
248 instructions of the Pierce™ Classic Magnetic IP/Co-IP Kit (Thermo Scientific,
249 Waltham, USA; Catalog number: 88804). In the lysis buffer, add ITGB4 antibody
250 (10μg; Proteintech), EZR antibody (10μg; Proteintech), and IgG antibody (10 μg;
251 Proteintech) respectively, and incubate at room temperature for 2 hours. Then, add the
252 magnetic beads to the lysate and rotate continuously for 1 hour to ensure thorough
253 mixing of the magnetic beads with the lysate. After that, use a magnetic stand to
254 collect the magnetic beads, wash the beads with the elution buffer, and add
255 neutralization buffer to adjust the pH to neutral. The obtained protein samples are then
256 subjected to Western blot analysis.

257 **Bioinformatics analysis**

258 The data on the mRNA expression of ITGB4 in the adjacent and cancerous tissues of
259 CRC patients comes from the TCGA (https://www.aclbi.com/static/index.html#/tcga)
260 and GEO (https://www.aclbi.com/static/index.html#/geo) databases. The
261 Kaplan-Meier (https://kmplot.com/analysis/) online website was used to analyze the
262 impact of gene expression levels on the prognosis of CRC patients. The gene
263 expression levels in colorectal cancer and adjacent normal tissues were analyzed in

264 GEPIA2 (http://gepia2.cancer-pku.cn/#index). The subcellular gene localization
265 analysis was obtained from the GeneCards (https://www.genecards.org/) website.

266 **Statistical analysis**

267 In this study, each experimental group was subjected to three independent replicate
268 experiments. Results of normally distributed data are expressed as mean ± standard
269 deviation, while data that is not normally distributed are represented by median and
270 interquartile range. Statistical analyses were conducted using GraphPad Prism 8.0
271 (GraphPad Software, La Jolla, CA, USA) and SPSS 21.0 (IBM, Armonk, NY, USA).
272 Statistical methods such as t-test, one-way ANOVA, and two-way ANOVA were
273 employed. A P-value of less than 0.05 was considered statistically significant,
274 indicating that the difference was statistically meaningful.

275 **Results**

276 **ITGB4 is upregulated in colorectal cancer patients and is associated with poor**
277 **prognosis.**

278 To validate the expression of ITGB4 in CRC tissues, we analyzed the expression of
279 ITGB4 in colorectal cancer tissues and adjacent normal tissues using the TCGA and
280 GEPIA2 databases. The results showed that the expression level of ITGB4 in cancer
281 tissues was higher than that in adjacent normal tissues (Figure 1 A-C). Kaplan-Meier
282 survival analysis revealed that patients with high ITGB4 expression had a poorer
283 overall survival compared to those with low ITGB4 expression in colorectal cancer
284 (Figure 1 D). This aligns with the previous research findings from our team, which
285 indicated that ITGB4 is highly expressed in the serum and tissues of CRC patients,

286 and that ITGB4 is associated with the overall survival of CRC patients. In summary,
287 ITGB4 is an oncogenic factor in colorectal cancer and is closely associated with poor
288 prognosis in patients with colorectal cancer. ITGB4 may serve as a potential tumor
289 marker for CRC patients.

290 **Downregulating ITGB4 inhibits the proliferation, migration, and invasion of**
291 **colorectal cancer and promotes apoptosis.**

292 In order to explore the mechanism of action of ITGB4 in CRC, we down-regulated
293 the expression of ITGB4 in SW480 and HCT116 cells to observe its effect on CRC
294 cell function. Firstly, four siRNA sequences targeting different sites of ITGB4 were
295 simultaneously transfected into SW480 cells. The knockdown efficiency at the mRNA
296 and protein levels was verified using qRT-PCR and Western Blot, respectively.
297 Among them, the siITGB4-681 sequence showed the most significant knockdown
298 efficiency, so siITGB4-681 was selected for subsequent experiments (Figure 2 A, B).
299 Next, after transfecting SW480 and HCT116 cells with siITGB4 and siNC, the
300 transfection efficiency was verified using qRT-PCR and Western Blot. The results
301 showed that both the mRNA (Figure 2 C, D) and protein (Figure 2 E, F) expression
302 levels were significantly reduced in the siITGB4 group. The CCK-8 cell proliferation
303 assay revealed that the cell proliferation capacity was significantly inhibited after
304 ITGB4 knockdown (Figure 2 G, H). The plate clone formation assay indicated that
305 the clone formation ability of the cells was significantly suppressed following ITGB4
306 knockdown (Figure 2 I, J). Flow cytometry analysis showed that the apoptosis rate in
307 the ITGB4 knockdown group was significantly higher than that in the control group

308 (Figure 2 K, L). Additionally, the Transwell migration and invasion assays
309 demonstrated that ITGB4 knockdown significantly reduced the cell migration and
310 invasion abilities (Figure 2 M, N). These results suggest that downregulating ITGB4
311 can inhibit the proliferation, migration, and invasion of CRC cells, and promote
312 apoptosis.

313 **ITGB4 inhibits the growth of colorectal cancer cells in vivo.**

314 To further validate the tumor-promoting role of ITGB4 in vivo in colorectal cancer
315 (CRC), a stable HCT116 cell line with shITGB4 transfection was constructed, and the
316 knockdown efficiency of ITGB4 was verified by qRT-PCR and Western blot (Figure 3
317 A, B). HCT116 cells stably transfected with shRNA-ITGB4 and shRNA (shITGB4
318 and shNC) were injected subcutaneously into two groups of nude mice to establish
319 tumor-bearing nude mouse models. The tumor size, weight, and growth curves for
320 both groups are shown in Figure 3 C-F. The results indicated that compared to the
321 shNC group, the shITGB4 group had a significantly reduced tumor growth rate,
322 volume, and weight. Subsequently, qRT-PCR and Western blot experiments were
323 conducted to verify the knockdown efficiency of ITGB4 in the xenograft tumor
324 tissues (Figure 3 G, H). Hematoxylin and eosin (HE) staining was used to evaluate the
325 morphological characteristics of the xenograft tumor tissues, and the results showed
326 that the cellular morphology and structure were similar to those of CRC tissues
327 (Figure 3 I). Ki-67 immunohistochemical staining revealed that the proliferation
328 capacity of cells in the shITGB4 group was significantly inhibited compared to the
329 shNC group (Figure 3 J, K). These findings collectively indicate that downregulating

330 ITGB4 can inhibit the growth of CRC in vivo and modulate the tumorigenic
331 properties such as proliferation and invasion of colon cancer cells.

332 **In colorectal cancer, ITGB4 regulates the expression of EZR**

333 In order to gain a deeper understanding of the potential role of ITGB4 in the
334 pathogenesis of colorectal cancer (CRC), RNA-seq analysis was performed on
335 SW480 cells transfected with siNC and siITGB4, respectively， The results showed
336 that after knockdown of ITGB4, the expression levels of 572 genes were significantly
337 altered, with 276 genes upregulated and 296 genes downregulated (Figure 4 A, B).
338 Among the downregulated genes, there were 35 genes with log2|Fold Change| > 1.0
339 and $P < 0.05$. Subsequently, this study will screen for genes co-expressed with ITGB4
340 in the GEPIA database, identify genes upregulated in CRC in the GEPIA2 database,
341 and overlap these with genes downregulated in association with ITGB4 expression
342 from the previous RNA-seq data. By conducting an overlap analysis, genes with a
343 P-value < 0.01 in the transcriptome sequencing results will be selected. Additionally,
344 by searching the GEPIA2 database and GeneCards website, genes with similar
345 subcellular localization to ITGB4 will be screened. Ultimately, five candidate target
346 genes are identified: ITGA6, CXADR, EZR, GPRC5C, and EPHA2 (Figure 4 C).
347 After knocking out ITGB4 in SW480 and HCT116 cells, the mRNA expression levels
348 of ITGA6, CXADR, EZR, GPRC5C, and EPHA2 genes were detected using
349 qRT-PCR. The results showed that the mRNA expression of these five candidate
350 genes was reduced (Figure 4 D, E). Subsequently, we further analyzed the data using
351 ChIPBase, the Kaplan-Meier Plotter online website, the GEPIA2 database, and

352 Pearson correlation analysis. The results indicated that the EZR gene has a closer
353 relationship with ITGB4 in terms of co-expression and subcellular localization, with a
354 more significant difference between cancerous and adjacent non-cancerous tissues.
355 Additionally, in colorectal cancer tissues, the expression of EZR was positively
356 correlated with ITGB4 expression (Figure 5A-C). The Kaplan-Meier survival analysis
357 of the five candidate genes revealed that patients with high expression of EZR had a
358 lower overall survival rate (Figure 5 D), which was consistent with the results for
359 ITGB4. Based on the aforementioned analyses, EZR was identified as a downstream
360 target gene of ITGB4.

361 **ITGB4 interacts with EZR in colorectal cancer, and ITGB4 targets and regulates**
362 **EZR.**

363 Next, to gain a deeper understanding of the molecular mechanism by which ITGB4
364 promotes tumor progression in colorectal cancer (CRC), we validated the interaction
365 between ITGB4 and EZR in SW480 cells through Co-IP (Co-immunoprecipitation)
366 and Co-IF (Co-immunofluorescence) experiments. The total protein from SW480
367 cells was immunoprecipitated with ITGB4 antibody and EZR antibody, and the
368 co-precipitation of ITGB4 and EZR in CRC cells was confirmed by Western blot
369 analysis (Figure 6 A). Subsequently, we further investigated the intracellular
370 localization of ITGB4 and EZR by immunofluorescence staining. Confocal
371 microscopy images revealed that ITGB4 and EZR are co-localized at the cell
372 membrane in CRC cells (Figure 6 B). The STRING online website, PPI
373 (Protein-Protein Interaction) map (Figure 6 C), further indicates that there is a

374 protein-protein interaction relationship between ITGB4 and EZR. Next, qRT-PCR and
375 Western blot methods were used to verify the transfection efficiency of the EZR
376 overexpression plasmid. The results showed that the expression levels of EZR mRNA
377 (Figure 6 D) and protein (Figure 6 E) in SW480 and HCT116 cells were significantly
378 increased, indicating that the constructed EZR overexpression plasmid successfully
379 upregulated the expression of EZR in SW480 and HCT116 cells. To further confirm
380 the regulation of ITGB4 on EZR expression in CRC cells, qRT-PCR and Western blot
381 methods were used to verify the changes in EZR mRNA and protein expression levels
382 after ITGB4 knockdown. The results showed that after ITGB4 knockdown in SW480
383 cells, the expression levels of EZR mRNA and protein significantly decreased (Figure
384 6 F, G). These results indicate that ITGB4 and EZR interact in CRC, and ITGB4 can
385 regulate EZR at both the mRNA and protein levels. Next, siRNA-NC/siRNA-ITGB4
386 and pcDNA3.1-vector/pcDNA3.1-EZR were separately and co-transfected into
387 SW480 and HCT116 cells. qRT-PCR was used to detect changes in ITGB4 mRNA
388 expression in each group. The results showed that the effect of ITGB4 knockdown on
389 the downregulation of mRNA expression levels could be attenuated by overexpressing
390 EZR (Figure 6 H). Similarly, Western blot was used to detect changes in ITGB4
391 protein expression levels in each group, and the results showed that the effect of
392 ITGB4 knockdown on protein expression could be weakened by overexpressing EZR
393 (Figure 6 I). These findings suggest that ITGB4 and EZR have an interactive
394 relationship in CRC cells, and ITGB4 can influence the expression of EZR in CRC
395 cells.

ITGB4 promotes the occurrence and development of colorectal cancer (CRC) by targeting the regulation of EZR to activate the Wnt/β-catenin signaling pathway.

To further elucidate the mechanism by which ITGB4 regulates downstream signaling pathways, KEGG enrichment analysis was performed on the co-expressed genes identified in the siITGB4 transcriptome sequencing. The results indicated that these genes were significantly enriched in the Wnt/β-catenin signaling pathway (Figure 7 A). Subsequently, the impact of ITGB4 knockout on the Wnt/β-catenin signaling pathway was verified using the Western blot method. The results indicate that when ITGB4 expression is downregulated in HCT116 cells, the expression levels of key proteins in the Wnt/β-catenin signaling pathway, including β-catenin, as well as its downstream target genes c-Myc and cyclinD1, are also significantly downregulated，The results indicate that ITGB4 can activate the Wnt/β-catenin signaling pathway. Additionally, the overexpression of EZR can rescue the downregulation of key proteins in this pathway caused by ITGB4 knockout (Figure 7 B). These findings demonstrate that EZR is involved in the activation of the Wnt/β-catenin signaling pathway by ITGB4. Next, to further explore the impact of the ITGB4/EZR axis on colorectal cancer (CRC), we conducted cell functional rescue experiments, The results indicate that knockdown of ITGB4 can decrease the proliferation, migration, and invasion capabilities of CRC cells, Overexpression of EZR can enhance the proliferation, migration, and invasion capabilities of CRC cells, Furthermore, the decrease in proliferation, migration, and invasion capabilities of CRC cells induced by ITGB4 knockdown can be restored by upregulating EZR (Figure 7 C-I). In summary,

418 EZR is a key downstream target gene for ITGB4 in promoting CRC progression, and
419 ITGB4 exerts its oncogenic effects by targeting the regulation of EZR to activate the
420 Wnt/β-catenin signaling pathway.

421 **Discussion**

422 This study confirms that ITGB4 is highly expressed in tumor tissues of CRC patients
423 and is associated with poor patient prognosis. The oncogenic role of ITGB4 in CRC
424 was further validated through in vitro and in vivo experiments. Moreover, this is the
425 first report of the downstream target gene EZR of ITGB4, which is regulated by
426 ITGB4 and affects various biological functions of CRC cells through the activation of
427 the Wnt/β-catenin signaling pathway, thereby promoting the occurrence and
428 development of CRC. This research reveals the clinical significance and potential
429 value of the ITGB4/EZR/Wnt/β-catenin axis in the treatment of CRC.

430 ITGB4, also known as integrin subunit beta 4, CD104, or GP150, is a
431 tumor-associated antigen (TAA). Its genomic location is at 17q25.1. It mediates the
432 connection or interaction between cells and the extracellular matrix, as well as
433 intercellular interactions, and plays a significant role in signal transduction [9]. Current
434 studies have found that ITGB4 is abnormally expressed in various cancers, including
435 lung cancer, pancreatic cancer, gastric cancer, and colorectal cancer, and may be
436 positively associated with poor prognosis [10-15]. Preliminary results from our research
437 group also indicate that ITGB4 is highly expressed in CRC tumor tissues and serum,
438 and ITGB4 is associated with prognostic factors of CRC [16]. These findings
439 collectively indicate that ITGB4 plays a promotional role in the occurrence and

development of colorectal cancer (CRC). In this study, the results of bioinformatics analysis indicate that the expression level of ITGB4 in CRC cancer tissues is higher than that in adjacent normal tissues, and colorectal cancer patients with high ITGB4 expression have a poorer overall survival. The abnormal expression of ITGB4 in CRC suggests that it may play a regulatory role in the occurrence and development of cancer.

TGB4 is involved in the regulation of various cellular functions, affecting the migration, invasion, proliferation, and survival of tumor cells, as well as regulating angiogenesis, connective tissue proliferation, and immune response in tumor host cells, thereby influencing epithelial-mesenchymal transition (EMT), cancer development, metastasis, and even treatment outcomes [17,18]. Studies have found that ITGB4 is highly expressed in gastric cancer cell lines and gastric cancer tissues, and overexpression of ITGB4 significantly promotes the invasion, migration, and proliferation capabilities of gastric cancer cell lines [19,20]. Another study confirmed that reducing the expression level of ITGB4 inhibits the proliferation, colony formation, and invasiveness of hepatocellular carcinoma cells, while overexpression of ITGB4 promotes the proliferation and invasiveness of hepatocellular carcinoma cells and induces epithelial-to-mesenchymal transition (EMT) [21]. Previous studies using xenograft mouse models have shown that a decrease in ITGB4 protein levels can inhibit the tumorigenicity of the BGC823 gastric cancer cell line [20]. To investigate the mechanism of action of ITGB4 in the progression of colorectal cancer, we conducted a series of in vitro cell functional experiments, Our preliminary

experiments have confirmed that ITGB4 is highly expressed in the HCT116 and SW480 cell lines, therefore, in this study, we selected these two cell lines to detect the biological functions of ITGB4. The research results indicate that downregulating the expression of ITGB4 significantly inhibits the proliferation, migration, and invasion of CRC cells, and promotes apoptosis. Additionally, in vivo experiments, we observed that the tumor growth rate, weight, and volume were all reduced in the nude mouse tumor model with low ITGB4 expression compared to the negative control group. The expression intensity of Ki67 in tumor tissue is closely related to the proliferation of tumor cells. In this study, the Ki67 positive expression rate was lower in the group with low ITGB4 expression, indicating that the absence of ITGB4 inhibits the proliferation of CRC tumor cells in vivo. This is consistent with previous research results, collectively indicating that ITGB4 plays a pro-oncogenic role in the occurrence and development of malignant tumors. In summary, these results demonstrate that ITGB4 can promote the occurrence and development of CRC tumor cells, acting as an oncogenic factor, and it holds promise as a novel therapeutic target for CRC treatment.

To further explore the downstream target genes regulated by ITGB4, RNA-seq and bioinformatics analysis were used to screen five candidate target genes. Among them, the EZR gene showed a closer relationship with ITGB4 in terms of co-expression and subcellular localization. In colorectal cancer tissues, the expression of EZR was positively correlated with ITGB4, and the difference between cancerous and adjacent non-cancerous tissues was more pronounced. The EZR (Ezrin) gene is located on

484 chromosome 6q25.2-q26 and is a key member of the ERM (ezrin-radixin-moesin)
485 family, being the first to be discovered. It is a transmembrane-cytoskeletal linking
486 protein, with its main structural body positioned inside the cell membrane. The EZR
487 protein regulates tumor differentiation, invasion, and metastasis by interacting with
488 adhesion molecules on the surface of cancer cells [22]. Previous studies have reported
489 that EZR is significantly upregulated in digestive system malignant tumors, especially
490 in those with early metastasis and rapid disease progression such as gastric cancer,
491 colorectal cancer, liver cancer, pancreatic cancer, biliary tract tumors, and esophageal
492 cancer [23-27]. The expression of EZR protein in tumors is significantly correlated with
493 the clinical grade, TNM stage, and lymph node metastasis of colorectal cancer. High
494 expression of EZR is significantly associated with poor prognosis in colorectal and
495 esophageal cancers. These studies confirm that EZR protein can serve as a potential
496 biomarker for the clinical diagnosis, recurrence, and prognosis assessment of
497 gastrointestinal malignant tumors [28]. In this study, bioinformatics analysis indicated
498 that EZR is highly expressed in CRC tumor tissues, and CRC patients with high EZR
499 expression have a lower overall survival rate. These findings are consistent with
500 previous results, suggesting that EZR may play a pro-tumorigenic role in the
501 occurrence, progression, and metastasis of CRC.

502 Subsequently, to further demonstrate the interaction between ITGB4 and EZR in
503 CRC cells, a Co-IP experiment was conducted in this study. The results showed that
504 ITGB4 and EZR could be co-precipitated in CRC cells. In the Co-IF experiment,
505 confocal microscopy images revealed that both proteins were co-localized on the cell

506 membrane in CRC cells. These findings confirm the interaction between ITGB4 and
507 EZR in CRC cells, a conclusion that has not been previously reported in existing
508 studies. In addition, bioinformatics analysis predicted an interaction between ITGB4
509 and EZR proteins, which further supports the aforementioned conclusion. Following
510 this, qRT-PCR and Western blot methods were used to confirm that ITGB4 can
511 regulate the expression of EZR at both the translational and transcriptional levels in
512 CRC cells, further indicating that ITGB4 targets the regulation of EZR expression in
513 CRC cells.
514 To further elucidate the mechanism by which ITGB4 regulates EZR to promote CRC
515 progression, KEGG gene pathway analysis was performed on genes co-expressed
516 with siITGB4 in transcriptome sequencing. The results indicated that these genes are
517 enriched in the Wnt/β-catenin signaling pathway. It can be inferred that the oncogenic
518 role of ITGB4 in colorectal cancer (CRC) may be mediated by targeting the
519 regulation of EZR and activating the Wnt/β-catenin signaling pathway. Previous
520 studies have confirmed that the loss of normal cell polarity and adhesion caused by
521 the activation of the Wnt/β-catenin signaling pathway is a fundamental step in tumor
522 progression and metastasis and is a driving force for many human cancers,
523 particularly colorectal cancer, hepatocellular carcinoma, and breast cancer [29]. The
524 activation of the Wnt/β-catenin signaling pathway involves Wnt signal transduction at
525 the cell membrane, the stabilization of β-catenin in the cytoplasm, and the activation
526 of Wnt-related target genes in the nucleus[30]. When β-catenin reaches a certain level
527 in the cytoplasm, it is transported into the nucleus, where it binds to TCF/LEF

528 transcription factors, initiating the transcription of downstream target genes such as
529 c-Myc, cyclin D1, Dickkopf-related protein 1, matrix metalloproteinase (MMP)-7,
530 axin 2, and others. This leads to abnormal cell proliferation and resistance to
531 apoptosis, thereby inducing tumor formation[31]. In this study, Western blot analysis
532 was used to validate the effects of ITGB4 knockdown on the proteins β-catenin and its
533 downstream target genes c-Myc and cyclin D1, in order to confirm the activation of
534 the Wnt/β-catenin signaling pathway. Simultaneously, the inhibitory effect of ITGB4
535 knockdown on the signaling pathway can be rescued by EZR, further demonstrating
536 that EZR can also activate this signaling pathway. The above results indicate that
537 ITGB4 and EZR influence the occurrence and development of colorectal cancer (CRC)
538 by activating the Wnt/β-catenin signaling pathway. Finally, we also conducted
539 functional rescue studies to further validate that ITGB4 affects the proliferation,
540 migration, and invasion capabilities of colorectal cancer (CRC) cells through targeted
541 regulation of EZR. In summary, ITGB4 influences the proliferation, migration, and
542 invasion capabilities of colorectal cancer (CRC) cells by targeting the regulation of
543 EZR and activating the Wnt/β-catenin signaling pathway. This indicates that the
544 ITGB4/EZR/Wnt/β-catenin axis may be involved in the occurrence and development
545 of CRC tumors.
546 Admittedly, there are certain limitations to our study. Firstly, the expression of EZR
547 was not validated in CRC tumor tissues and adjacent non-tumor tissues. Secondly, the
548 mechanism of action of EZR in CRC requires further in-depth investigation in
549 subsequent studies.

550 In conclusion, ITGB4 acts as an oncogenic factor in colorectal cancer (CRC). It
551 promotes the proliferation, migration, and invasion of CRC by regulating EZR and
552 activating the Wnt/β-catenin signaling pathway. ITGB4 may potentially serve as a
553 biomarker and therapeutic target for CRC.

554

555 **Funding**

556 This work was supported by Hebei Provincial Government-funded Provincial Medical
557 Excellent Talent Project (ZF2023025, ZF2024134, ZF2025045, ZF2025048,
558 ZF2025051, LS202208 and LS202212), Hebei Natural Science Foundation
559 (H2022206292, H2024206140), Key R&D Program of Hebei Province (223777103D
560 and 223777113D), Hebei Province County General Hospital Appropriate Health
561 Technology Promotion Project (20220018), Prevention and treatment of geriatric
562 diseases by Hebei Provincial Department of Finance (LNB202202, LNB201809 and
563 LNB201909), Spark Scientific Research Project of the First Hospital of Hebei
564 Medical University (XH202312 and XH201805), Hebei Province Medical Applicable
565 Technology Tracking Project (G2019035) and other projects of Hebei Province (1387
566 and SGH201501).

567

568 **CRediT authorship contribution statement**

569 **Wang Jing:** Conceptualization, Data curation, Formal analysis, Methodology,
570 Validation, Visualization, Writing – original draft, Writing – review & editing. **Yi Si:**
571 Conceptualization, Data curation, Formal analysis, Visualization, Writing – original

draft, Writing – review & editing. **Mingda Xuan:** Conceptualization, Data curation, Formal analysis, Visualization, Writing – original draft, Writing – review & editing. **Shuangshuang Han:** Formal analysis, Visualization, Writing – original draft. **Kunyi Liu:** Visualization, Writing – original draft. **Jiao Jiao:** Data curation, Writing – original draft. **Hongfei Li:** Formal analysis, Writing – original draft. **XiaoYan Men:** Formal analysis, Investigation Writing – original draft. **Weifang Yu:** Conceptualization, Funding acquisition, Project administration, Resources, Supervision, Writing – review & editing. **Ting Liu:** Conceptualization, Funding acquisition, Project administration, Validation, Writing – review & editing. **Jia Wang:** Conceptualization, Funding acquisition, Project administration, Resources, Supervision, Writing – review & editing.

Conflict Of Interest Statement

The authors have no conflicts of interest to declare.

References

1. Bray F, Laversanne M, Sung H, et al. Global cancer statistics 2022: GLOBOCAN estimates of incidence and mortality worldwide for 36 cancers in 185 countries. CA Cancer J Clin. 2024 May-Jun;74(3):229-263.

2. Zhang Y K, Xu C, et al. Progress in laparoscopic minimally invasive surgery for colorectal cancer [J]. Medical Review, 2021,27 (3): 582-591.

593 3. Gao Y, Chi P, Lin H M, et al. Prognostic impact of low number of lymph nodes
594 detected in neoadjuvant chemoradiadiation combined with surgery [J]. Chinese
595 Journal of Digestive Surgery, 2019,18 (8): 773-779.
596 4. Lao V V,Grady W M, et al. Epigenetics and Colorectal Cancer[J].Nat Rev
597 Gastroenterol Hepatol,2011,8(12):686-700.
598 5. Shuangshuang Han, Xia Jiang, Xiaofeng Sun, et al. Application value of CyTOF 2
599 mass cytometer technology at single-cell level in human gastric cancer cells.
600 Experimental Cell Research,2019,384(1): 111568.
601 6. Jiang X, Wang J, Wang M, et al. ITGB4 as a novel serum diagnosis biomarker and
602 potential therapeutic target for colorectal cancer. Cancer Med. 2021
603 Oct;10(19):6823-6834.
604 7. Zhang W, Zhang B, Vu T, et al. Molecular characterization of pro-metastatic
605 functions of β4-integrin in colorectal cancer. Oncotarget. 2017 Sep
606 27;8(54):92333-92345.
607 8. Zhong F, Lu HP, Chen G, et al. The clinical significance and potential molecular
608 mechanism of integrin subunit beta 4 in laryngeal squamous cell carcinoma. Pathol
609 Res Pract. 2020 Feb;216(2):152785.
610 9. Borradori L, Sonnenberg A, et al. Structure and function of hemidesmosomes: more
611 than simple adhesion complexes. J Invest Dermatol. 1999 Apr;112(4):411-8.
612 10. Desgrosellier JS, Cheresh DA, et al. Integrins in cancer: biological implications
613 and therapeutic opportunities. Nat Rev Cancer. 2010 Jan;10(1):9-22.

614 11. Boelens MC, van den Berg A, Vogelzang I, et al. Differential expression and
615 distribution of epithelial adhesion molecules in non-small cell lung cancer and normal
616 bronchus[J]. J Clin Pathol, 2007, 60:608-614.
617 12. Chung J, Bachelder RE, Lipscomb EA, et al. Integrin (alpha 6 beta 4) regulation
618 of eIF-4E activity and VEGF translation: a survival mechanism for carcinoma cells. J
619 Cell Biol. 2002 Jul 8;158(1):165-174.
620 13. Damhofer H, Medema JP, Veenstra VL, et al. Assessment of the stromal
621 contribution to Sonic Hedgehog-dependent pancreatic adenocarcinoma. Mol Oncol.
622 2013 Dec;7(6):1031-1042.
623 14. Gan L, Meng J, Xu M, et al. Extracellular matrix protein 1 promotes cell
624 metastasis and glucose metabolism by inducing integrin β4/FAK/SOX2/HIF-1α
625 signaling pathway in gastric cancer. Oncogene. 2018 Feb 8;37(6):744-755.
626 15. Ni H, Dydensborg AB, Herring FE, et al. Upregulation of a functional form of the
627 beta4 integrin subunit in colorectal cancers correlates with c-Myc expression.
628 Oncogene. 2005 Oct 13;24(45):6820-9.
629 16. Li M, Jiang X, Wang G, et al. ITGB4 is a novel prognostic factor in colon cancer.
630 J Cancer. 2019 Aug 28;10(21):5223-5233.
631 17. Wang L, Zhang X, Pang N, et al. Glycation of vitronectin inhibits VEGF-induced
632 angiogenesis by uncoupling VEGF receptor-2-αvβ3 integrin cross-talk. Cell Death
633 Dis. 2015 Jun 25;6(6):e1796.
634 18. Xiao T, Takagi J, Coller BS, et al. Structural basis for allostery in integrins and
635 binding to fibrinogen-mimetic therapeutics. Nature. 2004 Nov 4;432(7013):59-67.

636 19. Yang ZY, Jiang H, Qu Y, et al. Metallopanstimulin-1 regulates invasion and
637 migration of gastric cancer cells partially through integrin β4. Carcinogenesis. 2013
638 Dec;34(12):2851-2860.
639 20.Hong D, Zhang X, Li R, et al. Deletion of TMEM268 inhibits growth of gastric
640 cancer cells by down regulating the ITGB4 signaling pathway. Cell Death Differ.
641 2019 Aug;26(8):1453-1466.
642 21. Li J, Hao N, Han J, et al. ZKSCAN3 drives tumor metastasis via integrin
643 β4/FAK/AKT mediated epithelial-melancholy transition in hepatocellular carcinoma.
644 Cancer Cell Int. 2020 Jun 5;20:216.
645 22. Bretscher A. Fimbrin is a cytoskeletal protein that cross links F-actin in vitro. Proc
646 Natl Acad Sci U S A. 1981 Nov;78(11):6849-6853.
647 23. Lugini L, Lozupone F, Matarrese P, et al. Potent phagocyte activity discriminates
648 metastatic and primary human malignant melanomas: a key role of Ezrin. Lab Invest.
649 2003 Nov;83(11):1555-67.
650 24. Kim C, Shin E, Hong S, et al. Clinical value of Ezrin expression in primary
651 osteoarthritis. Cancer Res Treat. 2009 Sep;41(3):138-144.
652 25. Krishnan K, Bruce B, Hewitt S, et al. Ezrin mediates growth and survival in
653 Ewing's sarcoma through the AKT/mTOR, but not the MAPK, signaling pathway.
654 Clin Exp Metastasis. 2006;23(3-4):227-36.
655 26. Zhang Q, Ye Z, Zhang Y, et al. The Expression and Clinical Significance of Ezrin
656 and MMP-9 in Colorectal Cancer Tissue. Altern Ther Health Med. 2024 Jun
657 28:AT10725.

27. Yongpeng Diao , Qing Xu, Fei Li. Biological characteristics of Ezrin protein and its role in colorectal cancer metastasis [J]. Progress in Modern General Surgery in China, 2009,12:1074-1076.

28. Liang F, Wang Y, Shi L, et al. Association of Ezrin expression with the progression and prognosis of gastrointestinal cancer: a meta-analysis. Oncotarget. 2017 Oct 4;8(54):93186-93195.

29. Tejeda-Muñoz N, Mei KC, et al. Wnt signaling in cell adhesion, development, and colon cancer. IUBMB Life. 2024 Jul;76(7):383-396 .

30. Huang P,Yan R, Zhang X, et al. Activating Wnt/β-catenin signaling pathway for disease therapy: Challenges and opportunities. Pharmacol Ther. 2019;196:79–90.

31. Lin CH, Ji T, Chen CF, et al. Wnt signaling in osteosarcoma. Adv Exp Med Biol. 2014;804:33–45.

Table 1 The primer sequences

基因名	上游引物序列 5’-3’	下游引物序列 5’-3’
ITGB4	GCGACUACACUAUUGGAUUTT	AAUCCAAUAGUGUAGUCGCTT
EZR-1	ACCAATCAATGTCCGAGTTACC	GCCGATAGTCTTTACCACCTGA
β-actin	GAGTCAACGGATTTGGTCGT	CATGGGTGGAATCATATTGGA
EPHA2--1	TGGCTCACACACCCGTATG	GTCGCCAGACATCACGTTG
EPHA2--2	AGAGGCTGAGCGTATCTTCAT	GGTCCGACTCGGCATAGTAGA
EPHA2--3	ACTACGGCACCAACTTCCAG	GTAGAAGCCTTTGCGGGTGA
ITGA6--1	ATGCACGCGGATCGAGTTT	TTCCTGCTTCGTATTAACATGCT
ITGA6--2	GGCGGTGTTATGTCCTGAGTC	AATCGCCCATCACAAAAGCTC
ITGA6--3	CAGTGGAGCCGTGGTTTTG	CCACCGCCACATCATAGCC
CXADR	GTGCTCCTGTGCGGAGTAG	ATGGCAGATAGGCAGTTTCCC
EZR--2	AGCGGCTGATCCCTCAAAG	GGCATCAACTCCAAGCCAAAG
EZR--3	ATGCCCCACGTCTGAGAATC	TCCTGCGGCGCATATACAAC
GPRC5C--1	CCTGTACTACAACCTGTGTGAC	TGAGCACAAACGTGGTGACA
GPRC5C--2	CGTGGGCTATGAGACCATCC	CCGGCCTCTTAGCTGCAAC
GPRC5C--3	AAGAGGCCGGTGTCACCATA	CTCCTTCGGACGGAACTTTGT

687 **legend:**

688 **Figure 1. ITGB4 is upregulated in colorectal cancer patients and associated with**
689 **poor prognosis.** （**A-C**） The expression of ITGB4 in colorectal cancer tissues and
690 adjacent normal tissues was analyzed in the TCGA and GEPLA2 databases. **(D)**
691 Kaplan-Meier analysis of ITGB4 expression levels and overall survival in colorectal
692 cancer patients.

693 (A) **Figure 2. In colorectal cancer cells, knockdown of ITGB4 inhibits the**
694 **proliferation, migration, and invasion of colorectal cancer cells, and enhances the**
695 **apoptosis capability.** In SW480 cells, **(A)** the mRNA levels of four siITGB4
696 sequences were verified using qRT-PCR. **(B)** The protein expression levels of four
697 siITGB4 sequences were verified using Western blot. In SW480 and HCT116 cells,
698 **(C, D)** qRT-PCR was used to verify the knockdown efficiency of siITGB4 at the
699 mRNA level. **(E, F)** Western blot was used to verify the knockdown efficiency of
700 siITGB4 at the protein level. **(G, H)** The CCK-8 assay was used to detect the effect of
701 ITGB4 knockdown on the proliferation of SW480 and HCT116 cells. **(I, J)** The plate
702 colony formation assay was used to detect the effect of ITGB4 knockdown on the
703 cloning ability of SW480 and HCT116 cells. **(K, L)** Flow cytometry was used to
704 detect the effect of ITGB4 knockdown on the apoptosis of SW480 and HCT116 cells.
705 **(M, N)** Transwell migration and Transwell invasion assays were used to detect the
706 effect of ITGB4 knockdown on the migration and invasion abilities of SW480 and
707 HCT116 cells. (Crystal violet staining 200×) *P < 0.05, **P < 0.01, ***P < 0.001.

708 **Figure 3. The effect of ITGB4 on the growth of colorectal cancer in vivo. (A, B)**
709 qRT-PCR and Western blot experiments were used to verify the knockdown efficiency

710 of shITGB4 stable lines in HCT116 cells. **(C)** Nude mouse tumor-beaYONGring
711 model. **(D)** Tumor growth curve. **(E, F)** Images and weight of xenografted tumors
712 were analyzed. **(G, H)** Verification of the ITGB4 knockdown efficiency in xenograft
713 tumor tissues. **(I)** Representative images of tumor tissue sections stained with HE.
714 Scale bar, 50 μm. **(J，K)** Representative image of Ki67 IHC staining in tumor tissue
715 sections. Scale bar, 50 μm. Data are shown as means ± SD. $^{**}P$ <0.01, $^{****}P$
716 <0.0001

717 **Figure 4. ITGB4 Target Gene Screening.** Transcriptome sequencing results
718 analysis. **(A)** Heatmap of differentially expressed genes (DEGs) identified by
719 RNA-seq. **(B)** Number of DEGs identified by RNA-seq.**(C)** Screening of 5 candidate
720 target genes. **(D, E)** Validation of mRNA levels of the 5 candidate target genes after
721 ITGB4 knockdown in SW480 and HCT116 cells.

722 **Figure 5. Analysis of candidate genes in GeneCards, ChIPBase online website,**
723 **and TCGA, GEPIA2 databases. (A)** Subcellular localization of ITGB4 and the 5
724 candidate target genes on the GeneCards website. **(B)** Expression of ITGB4 and the 5
725 candidate genes in CRC cancer and adjacent tissue in the TCGA and GEPIA2
726 databases.**(C)** Co-expression relationship between the 5 candidate genes and ITGB4
727 on the ChIPBase website. **(D)** Kaplan-Meier survival analysis of ITGB4 and the 5
728 candidate target genes in colorectal cancer patients.

729 **Figure 6. TGB4 can bind to EZR and affect its protein and mRNA expression. (A)**
730 In SW480 cells, the protein-protein interaction between ITGB4 and EZR was verified
731 by Co-IP experiment. **(B)** In SW480 cells, the co-localization relationship between
732 ITGB4 and EZR was verified by Co-IF experiment. **(C)** Protein-protein interaction
733 map from the STRING online website. **(D, E)** In SW480 and HCT116 cells, the

734 transfection efficiency of pcDNA3.1-EZR was verified by qRT-PCR and Western
735 blot, respectively. **(F)** In SW480 cells, the expression of EZR mRNA was detected by
736 qRT-PCR after ITGB4 knockdown. **(G)** In SW480 cells, the expression of EZR
737 protein was detected by Western blot after ITGB4 knockdown. After co-transfection
738 of siITGB4 and pcDNA3.1-EZR in SW480 and HCT116 cells, **(H)** The expression of
739 ITGB4 mRNA and EZR mRNA in each group was detected by qRT-PCR. **(I)** The
740 expression of ITGB4 and EZR proteins in each group was detected by Western blot.
741 *P < 0.05, **P < 0.01, ***P < 0.001.

742 **Figure 7. Oncogenic function of ITGB4 depends on EZR and Wnt/β-catenin**
743 **signaling pathway. (A)** KEGG enrichment result of the genes coexpressed with
744 ITGB4 in CRC. **(B)** The expression levels of Wnt/β-catenin signaling pathway related
745 proteins were detected by Western blot after transient co-transfection of ITGB4
746 siRNA and EZR overexpression plasmid in HCT116 cells. **(C)** In SW480 and
747 HCT116 cells, the effect of EZR overexpression on the cell proliferation ability
748 induced by ITGB4 knockdown was detected by CCK-8 assay. In SW480 and
749 HCT116 cells, the effect of EZR overexpression on the cell migration ability induced
750 by ITGB4 knockdown was elucidated by wound healing assay **(D-G)** (200×
751 magnification) and Transwell migration assay (H, I) (crystal violet staining, 200×
752 magnification). **(J, K)** In SW480 and HCT116 cells, the effect of EZR overexpression
753 on the cell invasion ability induced by ITGB4 knockdown was elucidated by
754 Transwell invasion assay (crystal violet staining, 200× magnification). *P < 0.05, **P
755 < 0.01, ***P < 0.001.

Figure 1

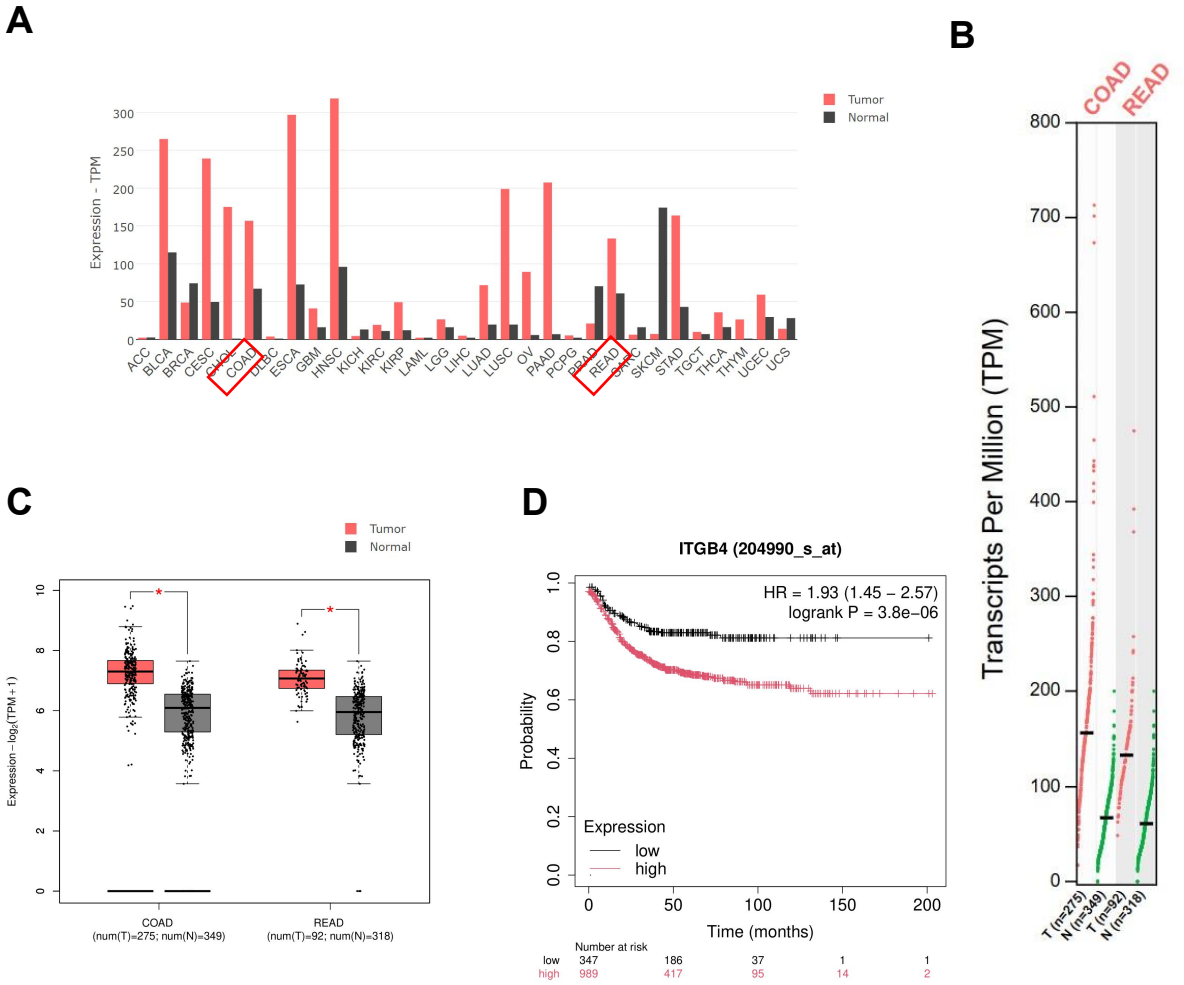
A
Tumor
Normal
Expression - TPM
ACC
BLCA
BRCA
CESC
CHOL
COAD
DLBC
ESCA
GBM
HNSC
KICH
KIRC
KIRP
LAML
LGG
LIHC
LUAD
LUSC
OV
PAAD
PCPG
PRAD
READ
SARC
SKCM
STAD
TGCT
THCA
THYM
UCEC
UCS
B
COAD
READ
Transcripts Per Million (TPM)
T (n=275)
N (n=349)
T (n=92)
N (n=318)
C
Tumor
Normal
Expression – log2(TPM + 1)
COAD
(num(T)=275; num(N)=349)
READ
(num(T)=92; num(N)=318)
D
ITGB4 (204990_s_at)
HR = 1.93 (1.45 – 2.57)
logrank P = 3.8e–06
Probability
Expression
low
high
Time (months)
Number at risk
low 347 186 37 1 1
high 989 417 95 14 2

Figure 2

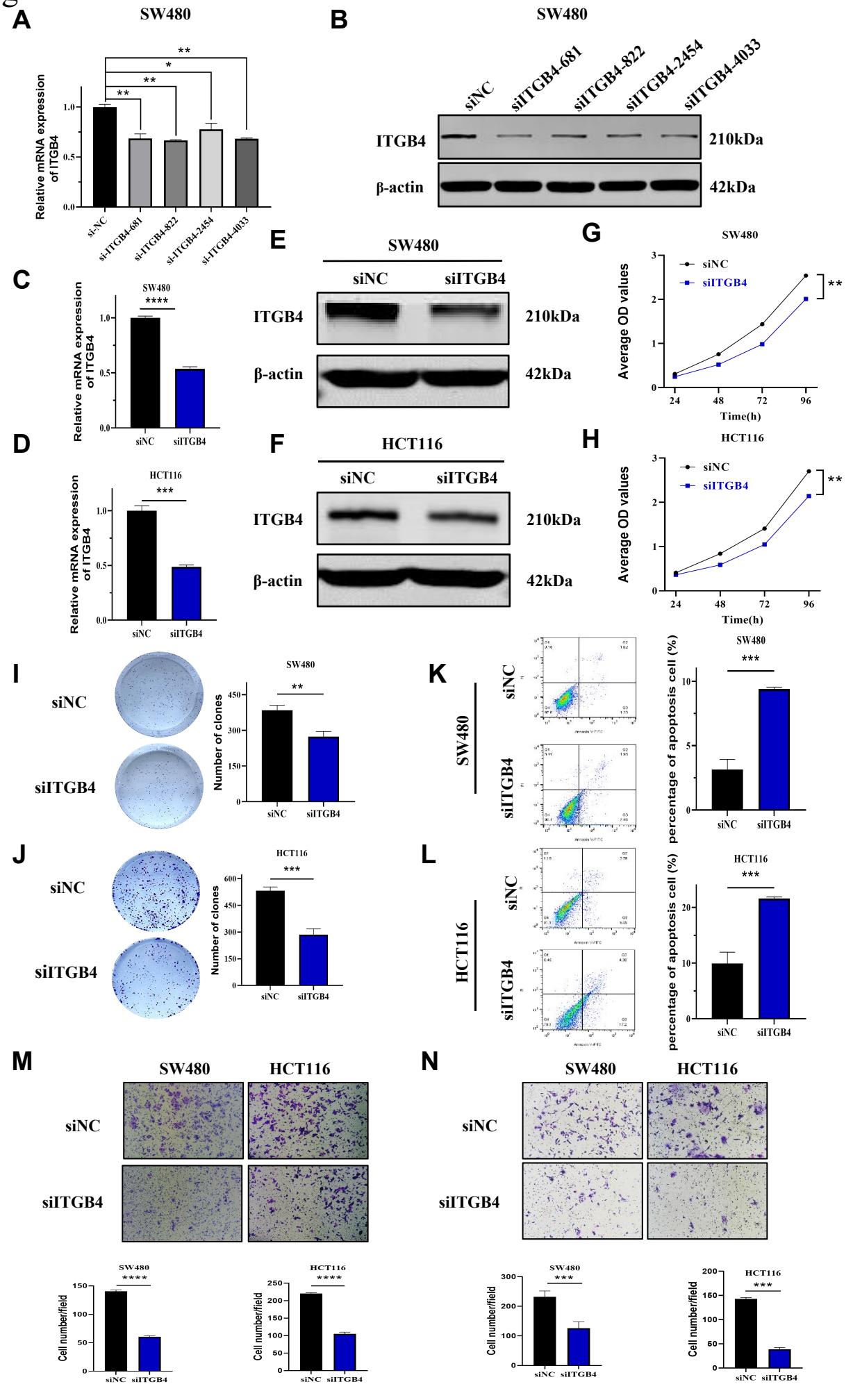
A
SW480
Relative mRNA expression of ITGB4
si-NC
si-ITGB4-681
si-ITGB4-822
si-ITGB4-2454
si-ITGB4-4033
B
SW480
siNC
siITGB4-681
siITGB4-822
siITGB4-2454
siITGB4-4033
ITGB4
β-actin
210kDa
42kDa
C
SW480
D
HCT116
E
SW480
siNC
siITGB4
F
HCT116
G
SW480
Average OD values
Time(h)
H
HCT116
I
SW480
Number of clones
J
HCT116
K
SW480
percentage of apoptosis cell (%)
L
HCT116
M
SW480
HCT116
Cell number/field
N

Figure 3

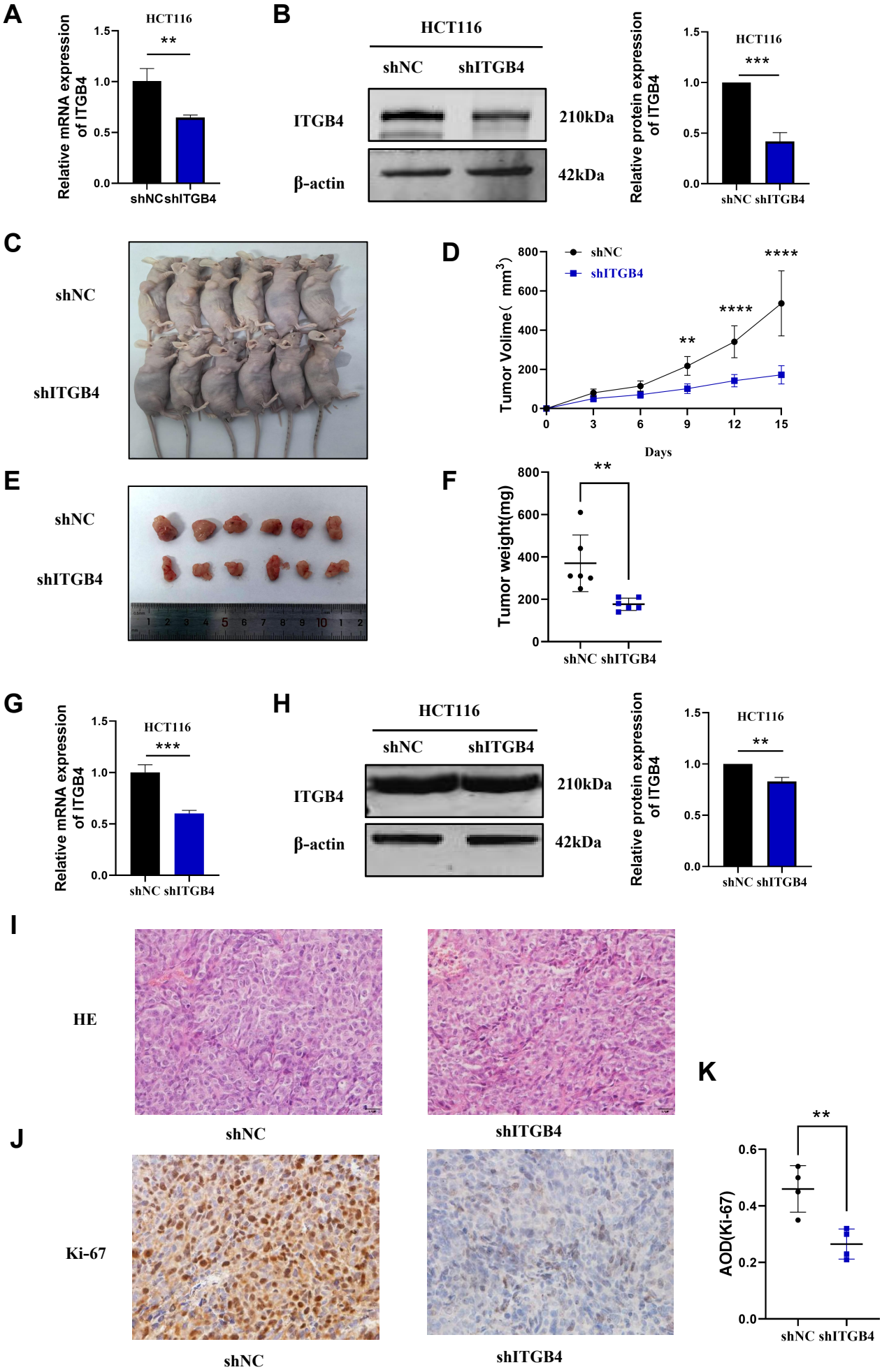
A
HCT116
**
Relative mRNA expression of ITGB4
1.5
1.0
0.5
0.0
shNC shITGB4
B
HCT116
shNC
shITGB4
ITGB4
210kDa
β-actin
42kDa
Relative protein expression of ITGB4
HCT116
***
shNC shITGB4
C
shNC
shITGB4
D
shNC
shITGB4
Tumor Volime（ mm3）
800
600
400
200
0
0
3
6
9
12
15
Days
**
****
****
E
shNC
shITGB4
F
Tumor weight(mg)
**
shNC shITGB4
G
HCT116
***
Relative mRNA expression of ITGB4
shNC shITGB4
H
HCT116
shNC
shITGB4
ITGB4
210kDa
β-actin
42kDa
Relative protein expression of ITGB4
HCT116
**
shNC shITGB4
I
HE
shNC
shITGB4
J
Ki-67
shNC
shITGB4
K
**
AOD(Ki-67)
0.6
0.4
0.2
0.0
shNC shITGB4

Figure 4

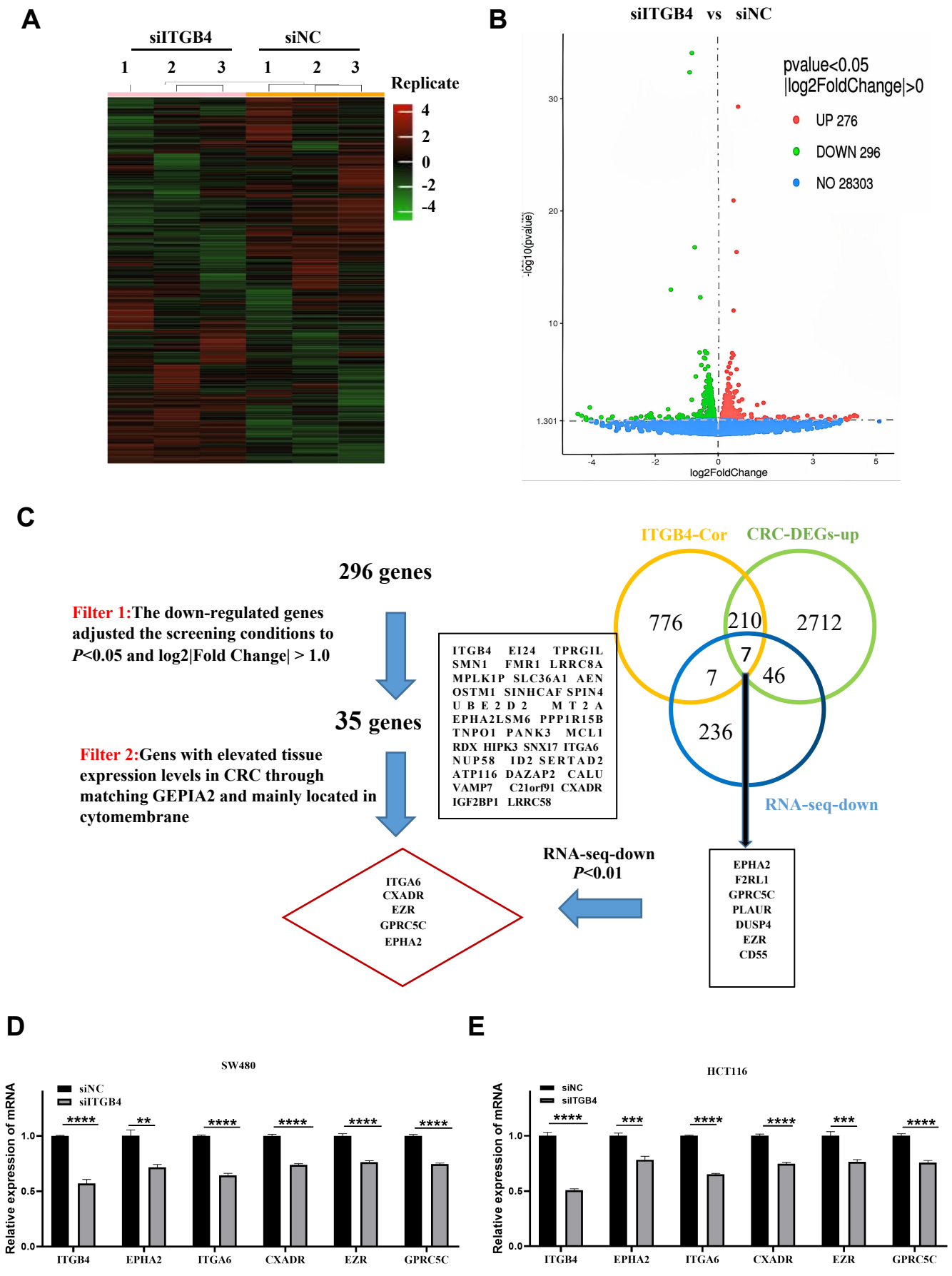
A
siITGB4
siNC
1 2 3 1 2 3
Replicate
4
2
0
-2
-4
B
siITGB4 vs siNC
pvalue<0.05
|log2FoldChange|>0
UP 276
DOWN 296
NO 28303
-log10(pvalue)
log2FoldChange
C
296 genes
Filter 1:The down-regulated genes adjusted the screening conditions to P<0.05 and log2|Fold Change| > 1.0
35 genes
Filter 2:Gens with elevated tissue expression levels in CRC through matching GEPIA2 and mainly located in cytomembrane
ITGB4 EI24 TPRGIL SMN1 FMR1 LRRC8A MPLK1P SLC36A1 AEN OSTM1 SINHCAF SPIN4 UBE2D2 MT2A EPHA2LSM6 PPP1R15B TNPO1 PANK3 MCL1 RDX HIPK3 SNX17 ITGA6 NUP58 ID2 SERTAD2 ATP116 DAZAP2 CALU VAMP7 C21orf91 CXADR IGF2BP1 LRRC58
ITGB4-Cor
CRC-DEGs-up
776
210
2712
7
7
46
236
RNA-seq-down
EPHA2
F2RL1
GPRC5C
PLAUR
DUSP4
EZR
CD55
RNA-seq-down
P<0.01
ITGA6
CXADR
EZR
GPRC5C
EPHA2
D
SW480
siNC
siITGB4
Relative expression of mRNA
ITGB4
EPHA2
ITGA6
CXADR
EZR
GPRC5C
E
HCT116
siNC
siITGB4
Relative expression of mRNA
ITGB4
EPHA2
ITGA6
CXADR
EZR
GPRC5C

Figure 5

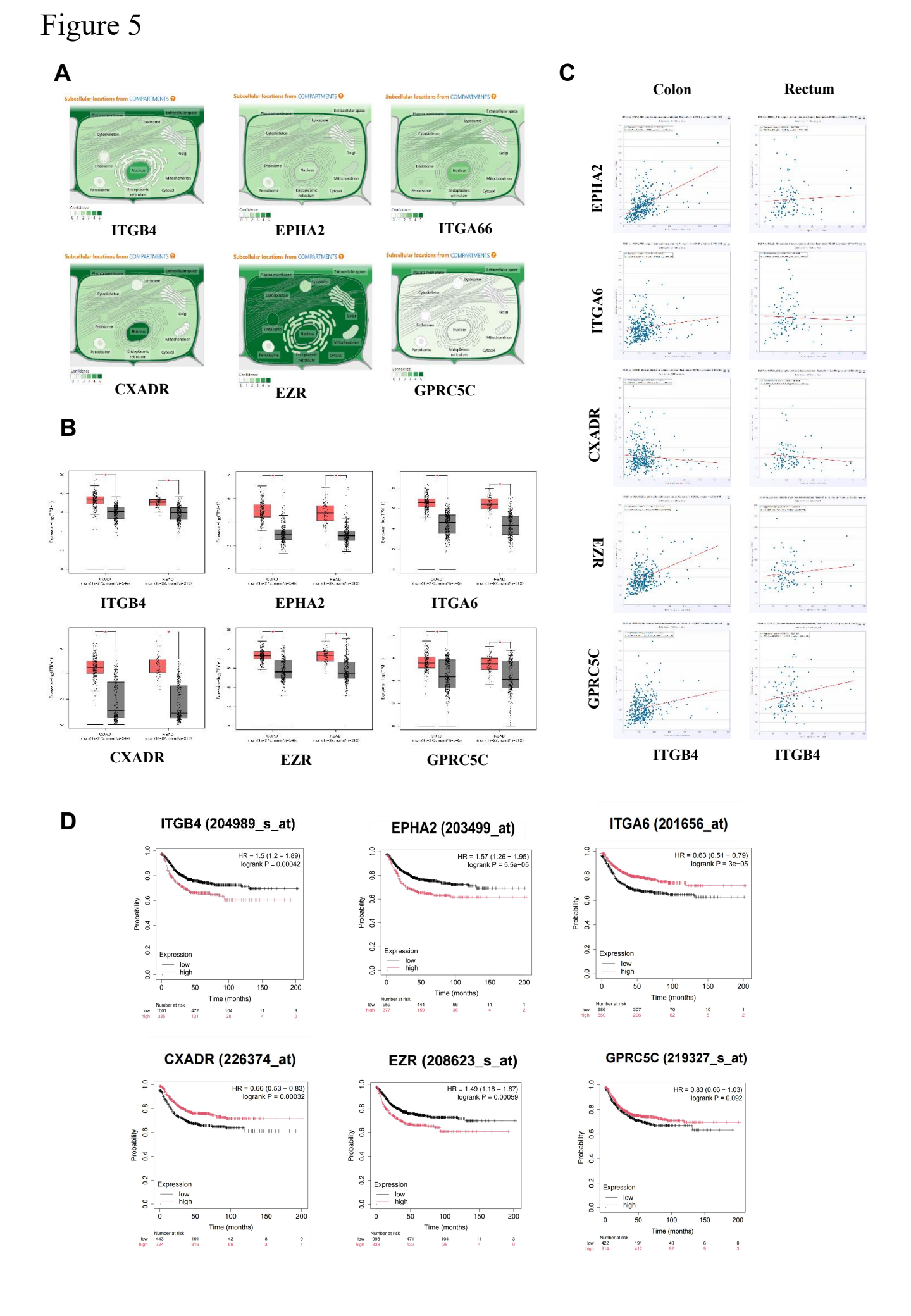
A
Subcellular locations from COMPARTMENTS
ITGB4
EPHA2
ITGA66
CXADR
EZR
GPRC5C
B
ITGB4
EPHA2
ITGA6
CXADR
EZR
GPRC5C
C
Colon
Rectum
EPHA2
ITGA6
CXADR
EZR
GPRC5C
ITGB4
ITGB4
D
ITGB4 (204989_s_at)
HR = 1.5 (1.2 − 1.89)
logrank P = 0.00042
EPHA2 (203499_at)
HR = 1.57 (1.26 − 1.95)
logrank P = 5.5e−05
ITGA6 (201656_at)
HR = 0.63 (0.51 − 0.79)
logrank P = 3e−05
CXADR (226374_at)
HR = 0.66 (0.53 − 0.83)
logrank P = 0.00032
EZR (208623_s_at)
HR = 1.49 (1.18 − 1.87)
logrank P = 0.00059
GPRC5C (219327_s_at)
HR = 0.83 (0.66 − 1.03)
logrank P = 0.092
Probability
Time (months)
Expression
low
high
Number at risk

Figure 6

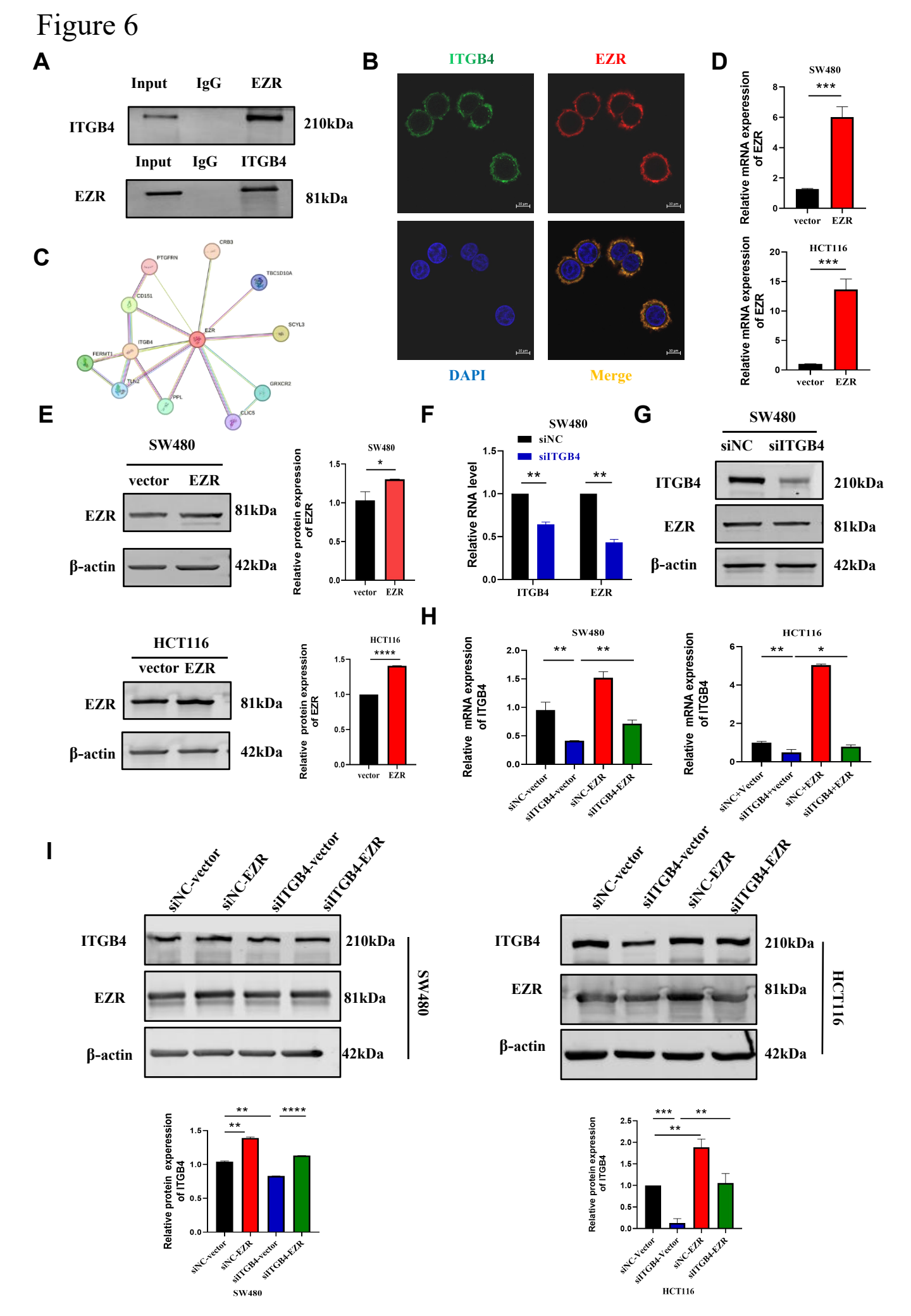
A
Input
IgG
EZR
ITGB4
210kDa
Input
IgG
ITGB4
EZR
81kDa
B
ITGB4
EZR
DAPI
Merge
C
CRB3
PTGFRN
TBC1D10A
CD151
SCYL3
EZR
ITGB4
FERMT1
TLN2
PPL
GRXCR2
CLIC5
D
SW480
***
Relative mRNA expression of EZR
vector
EZR
HCT116
***
Relative mRNA expression of EZR
vector
EZR
E
SW480
vector
EZR
EZR
81kDa
β-actin
42kDa
SW480
*
Relative protein expression of EZR
vector
EZR
F
SW480
siNC
siITGB4
**
**
Relative RNA level
ITGB4
EZR
G
SW480
siNC
siITGB4
ITGB4
210kDa
EZR
81kDa
β-actin
42kDa
HCT116
vector
EZR
EZR
81kDa
β-actin
42kDa
HCT116
****
Relative protein expression of EZR
vector
EZR
H
SW480
**
**
Relative mRNA expression of ITGB4
siNC-vector
siITGB4-vector
siNC-EZR
siITGB4-EZR
HCT116
**
*
Relative mRNA expression of ITGB4
siNC+Vector
siITGB4+vector
siNC+EZR
siITGB4+EZR
I
siNC-vector
siNC-EZR
siITGB4-vector
siITGB4-EZR
ITGB4
210kDa
EZR
81kDa
β-actin
42kDa
SW480
siNC-vector
siITGB4-vector
siNC-EZR
siITGB4-EZR
ITGB4
210kDa
EZR
81kDa
β-actin
42kDa
HCT116
**
**
****
Relative protein expression of ITGB4
siNC-vector
siNC-EZR
siITGB4-vector
siITGB4-EZR
SW480
***
**
**
Relative protein expression of ITGB4
siNC-Vector
siITGB4-Vector
siNC-EZR
siITGB4-EZR
HCT116

Figure 7

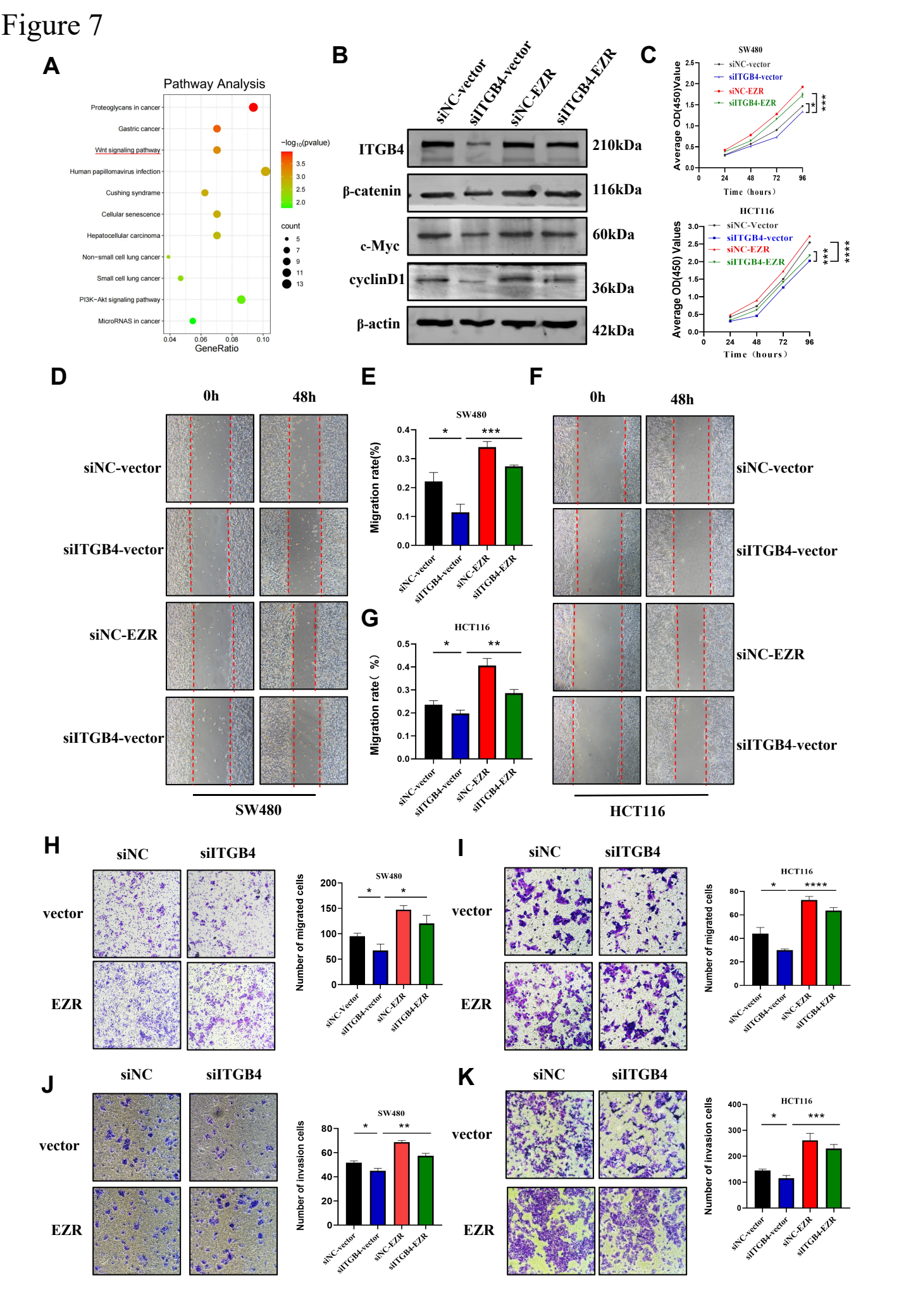
A
Pathway Analysis
Proteoglycans in cancer
Gastric cancer
Wnt signaling pathway
Human papillomavirus infection
Cushing syndrome
Cellular senescence
Hepatocellular carcinoma
Non-small cell lung cancer
Small cell lung cancer
PI3K-Akt signaling pathway
MicroRNAS in cancer
GeneRatio
-log10(pvalue)
count
B
siNC-vector
siITGB4-vector
siNC-EZR
siITGB4-EZR
ITGB4
β-catenin
c-Myc
cyclinD1
β-actin
210kDa
116kDa
60kDa
36kDa
42kDa
C
SW480
HCT116
Average OD(450)Value
Time (hours)
D
0h
48h
siNC-vector
siITGB4-vector
siNC-EZR
siITGB4-vector
SW480
E
Migration rate(%)
F
G
Migration rate (%)
HCT116
H
siNC
siITGB4
vector
EZR
Number of migrated cells
I
J
Number of invasion cells
K